COMPARISON OF $^{11}B^+$ AND $^{49}BF_2^+$ AT LOW IMPLANTATION ENERGY IN GERMANIUM PREAMORPHIZED SILICON.

Michel MINONDO[a], Claude JAUSSAUD[a], Dominique ROCHE[a], Anne-Marie PAPON[a], Peter VAN DER MEULEN[b], Sandeep MEHTA[b]

[a]LETI (CEA – Technologies Avancées), DMEL CEN/G – 85 X – F38041, Grenoble CEDEX, FRANCE
[b]Varian Ion Implant Systems, 35 Dory Road, Gloucester, MA01945, USA

The purpose of this work is to compare $^{11}B^+$ and $^{49}BF_2^+$ implantations for the formation of shallow (<0.1 μm) p^+/n junctions. In one hand, $^{49}BF_2^+$ implants can lead to higher sheet resistance than $^{11}B^+$ implants due to the presence of fluorine. In the other hand, boron enhanced diffusion is less important in presence of fluorine which would lead to shallower junctions. For this comparison, $^{11}B^+$ and $^{49}BF_2^+$ implants were done into crystalline and preamorphized silicon wafers and the results were analyzed by SIMS, Spreading Resistance and TEM. The implants of $^{11}B^+$ and $^{49}BF_2^+$ into Ge preamorphized Si followed by RTA allow to form junctions <0.1 μm, without any defect visible by TEM.

INTRODUCTION

Future 0.25 μm CMOS devices will require the use of very shallow p^+/n junctions, with a junction depth of less than 0.1 μm. The formation of shallow junctions requires both the use of a low energy boron implant and rapid thermal annealing (RTA), to reduce diffusion. The common solution to get a low energy boron implant is to use implantations with $^{49}BF_2^+$, which allows for a higher beam current and throughput as compared to direct extraction of boron at the lower energy. However, the present generation of modern implanters allows the direct use of low energy boron in a production scale.

The disadvantage of the use of BF_2 is that the presence of fluorine leads to a higher sheet resistance [1]. So an attractive solution is to use boron implantation at low energies, which would avoid the higher sheet resistance.

Low energy boron has a very wide acceptance angle for channeling, to the extent that even an oxide layer and orientation away from the major channeling directions and planes, is not sufficient to suppress channeling effects. As a result, a preamorphization implant is required to prevent the boron from going deep into the substrate. A good overview of channeling effects in boron implantation is given by Schreutelkamp et al. [2].

Preamorphization can be done with different species, such as Ar, Si, F, or Ge. Germanium because of its high mass, leads to quicker amorphization at lower doses, and a sharper crystalline-to-amorphous interface, leading to a smaller defective zone than the other species [3].

In addition, in the case of boron implant, the presence of germanium (which has an atomic radius larger than that of silicon) can reduce the stress induced by boron (atomic radius smaller than that of silicon). This compensation can help in eliminating the end-of-range defects [1].

The depth of preamorphization must be matched to the depth of the implanted boron profile :

- too shallow preamorphization leads to residual channeling effects,
- too deep preamorphization leads to residual end-of-range defects in the space charge region of the p^+/n junction which creates junction leakage.

The presence of fluorine, the condition of preamorphization and the presence of an oxide, can have an influence on the boron diffusion (normal or enhanced) during subsequent rapid thermal anneal [4]. For all these reasons, we studied the influence of the preamorphization and the presence of fluorine on boron diffusion.

EXPERIMENTAL

Wafer substrates were 100 mm <100> 14-22 Ω-cm Czochralski grown p-type. The reason for choosing p-type wafers is that subsequent spreading resistance measurements do not suffer from an effect known as carrier spilling [5]. Carrier spilling would

lead to an incorrect determination of the junction depth. On the other hand, substrate type has no influence on SIMS measurements.

The wafers were covered with a 55 Å thermal oxide, identical to the gate oxides used in 0.25 μm device technology. Germanium was implanted in some of the samples, at 30 keV, 10^{15} cm^{-2}, using backside wafer cooling, to prevent recrystallization during the implantation. This leads to a 550 Å amorphized layer, with a sharp crystalline to amorphous interface, which is sufficiently deep to contain all of the implanted boron profile.

The other samples were implanted directly into crystalline silicon, again covered with a 55 Å oxide.

Low energy boron (3 keV, $^{11}B^+$, 10^{15} cm^{-2}) and BF_2 (15 keV, $^{49}BF_2^+$, 10^{15} cm^{-2}) implants were performed on a Varian E500 high energy, medium current ion implanter [6]. This implanter has a variable extraction and acceleration/deceleration capability, which allows for the optimization of beam current and beam energy purity. We selected an extraction voltage of 7 kV and a deceleration of 4 kV for the boron implants (30 kV and 15 kV respectively for BF_2).

Typical end station pressure during implantation was in the order of 3 x 10^{-7} Torr. Therma-wave measurements [7], have shown that these settings cause undetectable levels of energy contamination by neutrals. All the wafers were implanted at a 0° implant angle.

Rapid Thermal Annealing (RTA) was done on a RRA ADDAX equipment at 950°C for 15s or at 1000°C for 10s in a nitrogen ambient. The wafer had a 8000 Å, SiO_2, PECVD cap.

Post implant analysis (before and after RTA) was performed on SIMS (CAMECA IMS300 with 5.5 keV Xe^+ primary beam). The depth accuracy of the SIMS measurements is estimated at 50 Å. In figure 1, we have shown SIMS profiles of the as-implanted samples. As is apparent from the figure, residual channeling appears clearly in the BF_2 implantation into the crystalline substrate and to a smaller extent, in the preamorphized samples. The residual channeling in the preamorphized samples can be explained by the shallow preamorphization depth (550 Å). Rutherford Backscattering Spectroscopy has shown that the BF_2 implant into crystalline silicon causes an amorphous layer of 300 Å for these conditions.

Spreading resistance profiles (SRP) were made on a SSM ASR 100 equipment. The samples were bevelled by using a 6-8 min angled mechanical grinding process.

Finally, some wafers were prepared for Cross-section Transmission Electron Microscopy (XTEM) which was performed on the [110] plan to enhance the visibility of residual damage.

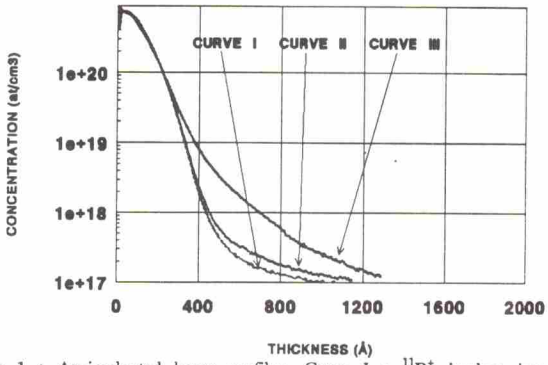

Fig 1 : As-implanted boron profiles. Curve I : $^{11}B^+$ implant into preamorphized Si. Curve II : $^{49}BF_2^+$ implant into preamorphized Si. Curve III : $^{49}BF_2^+$ implant into crystalline Si.

RESULTS

1. SIMS Measurements.

Figure 2a shows the results of SIMS analysis of the RTA at 950°C 15s, figure 2b contains the results for RTA at 1000°C 10s.

The B profiles in fig. 2a, already show the characteristic enhanced boron diffusion below the solid solubility limit of boron in Si [8]. The boron profiles show that the presence of fluorine during the RTA reduces the diffusion of boron (compare curves I -^{11}B into Ge preamorphized Si-, and II -BF_2 into Ge preamorphized Si) for concentration above 10^{18} cm^{-3}. This observation is in agreement with the work by Fan et al. [4].

Furthermore one can conclude from curves I and II that the diffusion of boron in the preamorphized sample was larger than in the crystalline sample (compare to curves II and III in fig. 1). This can be explained in terms of the presence of a larger amount of silicon interstitials, that are known to enhance boron diffusion [2].

Fig. 2b also shows that for the 1000°C 10 s anneal, the diffusion of boron is retarded by the fluorine. The solid solubility level at 1000°C is higher than at 950° C, which is the reason for enhanced diffusion

occurring between concentration levels of 10^{20} and 2×10^{20} cm^{-3}.

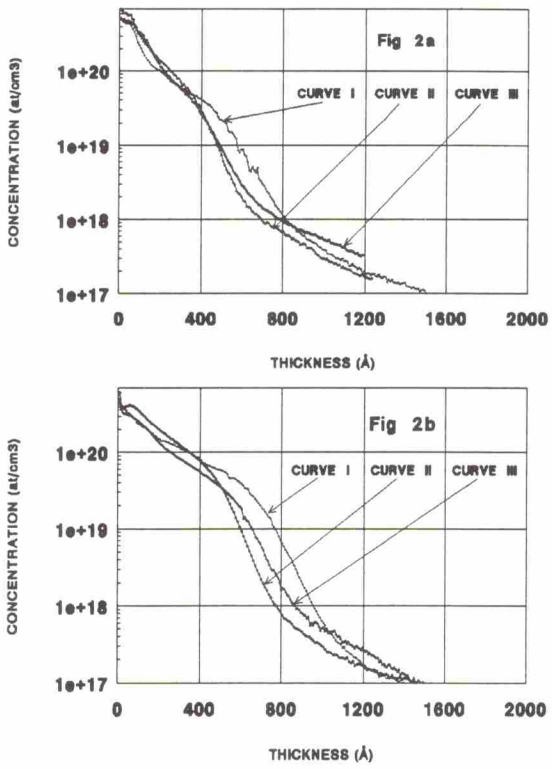

Fig 2 : Boron profiles after the annealing steps. a) anneal at 950°C/15s. b) anneal at 1000°C/10s. Curve I : $^{11}B^+$ implant into preamorphized Si. Curve II : $^{49}BF_2^+$ implant into preamorphized Si. Curve III : $^{49}BF_2^+$ implant into crystalline Si.

2. Spreading Resistance Measurements.

The same samples were characterized by spreading resistance measurement as shown in fig. 3 for a 950° C 15s RTA. This measurement technique allows to detect a lower dopant concentration than the SIMS measurements. As a result one can see that the implantation of BF_2 into crystalline Si has resulted in a deeper junction depth below a 10^{17} cm^{-3} (curve III in fig. 3a, junction depth 1500 Å at 10^{16} cm^{-3}) as compared to the other two profiles (1050 Å at 10^{16} cm^{-3}). The larger diffusion of B results obtained by SIMS (fig. 2a) are confirmed by the SRP measurements above 10^{18} cm^{-3}, where the ^{11}B implant again shows a larger diffusion. The results after the 1000°C/10s anneal are essentially the same as for the 950°C anneal. Preamorphization seems to be essential to prevent the formation of a deeper junction (curve III in fig. 3a), which is most likely caused by residual channeling of boron component of

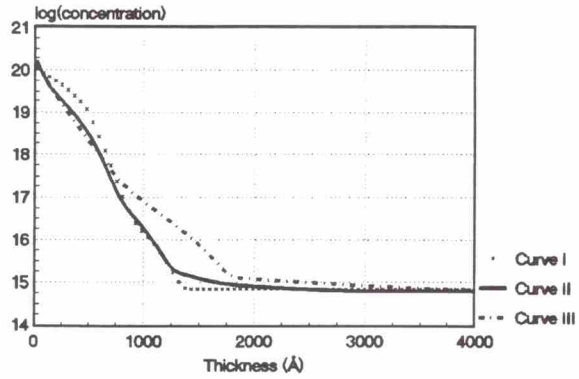

Figure 3 : SR profile after a 950 °C/15 s anneal. Curve I : $^{11}B^+$ implant into preamorphized Si. Curve II : $^{49}BF_2^+$ implant into preamorphized Si. Curve III : $^{49}BF_2^+$ implant into crystalline Si.

the $^{49}BF_2^+$ implant in the crystalline sample.

The comparison between SIMS and SRP shows that the channeling tail in BF_2^+ implanted into crystalline Si is electrically active, while it is not in the preamorphized samples. The reason for this difference is not clear.

3. XTEM Observations.

XTEM photographs are shown in fig. 4. Fig. 4a and 4b show the $^{49}BF_2^+$ implant into crystalline Si after annealing at 950°C and 1000°C respectively. One can see two types of defects : hairpin dislocations (stretching from the surface to about 300 Å depth), and dislocation loops (at a depth of 300 Å, diameter 130 Å). The damage depth distribution matches closely to the original amorphous – crystalline interface of 300 Å as measured by RBS. It seems that there are less dislocations after the 1000° C/10s annealing (density = 10^{10} cm^{-2}) than in the 950 °C/15s one (density = 2×10^{10} cm^{-2}).

Fig. 4c and 4d show the RTA results for the $^{11}B^+$ implants into Ge preamorphized Si. The sample with a 950°C RTA (Fig. 4c) shows a very low amount of defects, only dislocation loops are observed (10^8 cm^{-2}, depth 500 Å, diameter 130 Å). No defects are detected after 1000°C RTA (dislocation density < 10^6 cm^{-2}) showing that all the damages caused by the implantation dissolve for this RTA condition.

In figure 4e and 4f, the results of the $^{49}BF_2^+$ implants into preamorphized Si after RTA treatment at 950°C and 1000°C respectively are shown. No dislocation loops with a diameter larger than 20 Å were detected (density < 10^6 cm^{-2}). However, we can observe some bubbles (diameter : 20 Å,

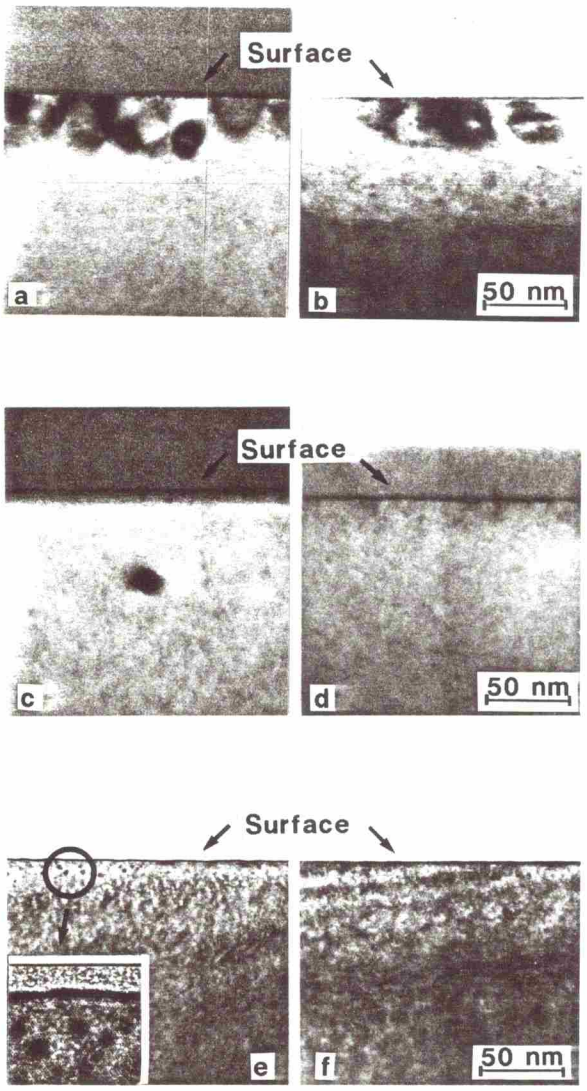

Fig 4 : XTEM observations. Fig 4a and 4b : $^{49}BF_2^+$ implant into crystalline Si at 950°C and 1000°°C respectively. Fig 4c and 4d : $^{11}B^+$ implant into preamorphized Si at 950°C and 1000°C respectively. Fig 4e and 4f : $^{49}BF_2^+$ implant into preamorphized Si at 950°C and 1000°C respectively. The inset in fig 4e shows the fluorine precipitates (magnification = 1 million).

stretching from the surface to 150 Å depth ; see the inset in fig 4e) which have been identified to be fluorine precipitates [9,10]. These precipitates were present in the $^{49}BF_2^+$ implant into crystalline Si but they were hidden by all the other numerous defects.

The best regrowth is observed for $^{49}BF_2^+$ implants into Ge preamorphized Si samples. It is conceivable that full regrowth can even be achieved at lower RTA temperatures.

DISCUSSION AND CONCLUSIONS

In the experiment described above, there are several things that play simultaneous roles :

- **Oxygen.** Since Czochralski wafers are used, the oxygen concentration is already high. This oxygen can be present as interstitial oxygen depending on thermal treatment. However during the implant, additional interstitial oxygen is generated by knock-in of oxygen from the 55 Å oxide layer. During the RTA, the oxygen precipitates as SiO_2, releasing Si interstitials. These Si interstitials will enhance the boron diffusion [11].
- **Preamorphization.** The preamorphization with Ge, results in the generation of a Si vacancy rich region near the surface ($< R_p$), and Si interstitials at depths $> R_p$ [12], which in turn enhances the diffusion of boron present in this region [13].
- **Fluorine.** Fluorine implants create more Si interstitials and this also would lead to enhanced boron diffusion. But, it has already been shown by Fan et al. [8] that the presence of fluorine decreases enhanced diffusion. The mechanism for this is presently unclear. However our experiments and those of Fan et al. seem to confirm this effect. A possible explanation given by K. Ohyu et al. [14], is that fluorine reduces the availability of Si interstitials.

The XTEM measurements indicate that the largest amount of post RTA damage is visible for the $^{49}BF_2^+$ implants into crystalline Si. This can be explained by the fact that for a Ge preamorphization the crystalline to amorphous interface is much sharper, and hence less defects are created behind the amorphous region, than compared to the $^{49}BF_2^+$ implant into crystalline Si. In the latter case, the recrystallization occurs from a very defective area, leading to a large amount of post RTA dislocations.

The presence of fluorine on the RTA of preamorphized Si helps in eliminating dislocations. As stated above, fluorine reduces the availability of silicon interstitials, which are at the origin of the formation of dislocations.

The presence of fluorine has benefits for both reducing enhanced boron diffusion, resulting in shallower junctions, and on the crystal regrowth, resulting in less demanding RTA. We have found a set of conditions (Ge 30 keV, 10^{15} cm^{-2} + BF_2^+ 15

keV, 10^{15} cm^{-2} + RTA 950°C 15s) that allow the formation of 0.1 μm junctions, without residual damage visible in standard conditions of TEM observations. These junctions can possibly even be achieved with a lower RTA temperature. Electrical characterization on diodes will follow in order to test the reverse leakage current on the samples formed with the different sets of conditions as stated above.

ACKNOWLEDGEMENTS

The authors would like to acknowledge Mr. B. Blanchard who performed the SIMS profiles.

REFERENCES

[1] A. Ferreiro, B. Biasse, A. M. Papon, J. Pontcharra, R. Truche, Nucl. Instr. Meth., **B39** (1989) 413–416.

[2] R.J. Schreutelkamp, J. S. Custer, V. Raineri, W. X. Lu, J. R. Liefting, F. W. Saris, K. T. F. Janssen, P. F. H. M. van der Meulen and R. E. Kaim, Mat. Sc. Eng., **B12** (1992) 307–325.

[3] T. Sands, J. Washburn, E. Myers and D. K. Sadana, Nucl. Instr. Meth., **B7/8** (1985) 337–341.

[4] D. Fan, J. M. Parks and R. J. Jaccodine, Appl. Phys. Lett., **59** (1992) 1212–1214.

[5] E.C. Andre, Jpn. J. of Appl. Phys., **30** (1991) 1511–1514.

[6] P.F.H.M. van der Meulen and R. Ammon, these proceedings.

[7] C. Jaussaud, F. Jourdan, A. Soubie, R. Simonton, these proceedings.

[8] C.P. Wu, J. T. McGinn and L. R. Hewitt, J. El. Mat., **18** (1989) 721–730.

[9] C. Carter, W. Maszara, D. K. Sadana, G. A. Rozgonyi, J. Liu and J. Wortman, Appl. Phys. Lett., **44** (1984) 459–461.

[10] C.H. Chu and L.J. Chen, Nucl. Instr. Meth. **B59/60** (1991) 391–394.

[11] D. Fan and R.J. Jaccodine, J. Appl. Phys., **67** (1990) 6135–6140.

[12] M. Servidori , R. Angelucci, F. Cembali, P. Negrini, S. Solmi, P. Zaumseil and U. Winter, J. Appl. Phys., **61** (1987) 1834–1849.

[13] Y.M. Kim , G. Q. Lo, H. Kinoshita, D. L. Kwong, H. H. Tseng and R. Hance, J. Electrochem. Soc., **138** (1991) 1122–1130.

[14] K. Ohyu, T. Itoga, and N. Natasuaki, Jpn . J. Appl. Phys. **29** (1990) 457–462.